

Article

Laboratory Study on Changes in the Pore Structures and Gas Desorption Properties of Intact and Tectonic Coals after Supercritical CO₂ Treatment: Implications for Coalbed Methane Recovery

Erlei Su ¹, Yunpei Liang ^{1,*}, Lei Li ^{1,2,3}, Quanle Zou ^{1,*} and Fanfan Niu ⁴

¹ State Key Laboratory of Coal Mine Disaster Dynamics and Control, Chongqing University, Chongqing 400044, China; suerlei1992@163.com (E.S.); leili80mky@163.com (L.L.)

² State Key Laboratory of Gas Disaster Monitoring and Emergency Technology, Chongqing 400037, China

³ China Coal Technology and Engineering Group Chongqing Research Institute, Chongqing 400037, China

⁴ Zhengzhou Engineering Co., Ltd. of China Railway Seventh Group, Zhengzhou 450052, China; niufanfan1991@163.com

* Correspondence: liangyunpei@cqu.edu.cn (Y.L.); quanlezou2016@cqu.edu.cn (Q.Z.)

Received: 31 October 2018; Accepted: 3 December 2018; Published: 6 December 2018



Abstract: Tectonic coals in coal seams may affect the process of enhanced coalbed methane recovery with CO₂ sequestration (CO₂-ECBM). The main objective of this study was to investigate the differences between supercritical CO₂ (ScCO₂) and intact and tectonic coals to determine how the ScCO₂ changes the coal's properties. More specifically, the changes in the tectonic coal's pore structures and its gas desorption behavior were of particular interest. In this work, mercury intrusion porosimetry, N₂ (77 K) adsorption, and methane desorption experiments were used to identify the difference in pore structures and gas desorption properties between intact and tectonic coals after ScCO₂ treatment. The experimental results indicate that the total pore volume, specific surface area, and pore connectivity of tectonic coal increased more than intact coal after ScCO₂ treatment, indicating that ScCO₂ had the greatest influence on the pore structure of the tectonic coal. Additionally, ScCO₂ treatment enhanced the diffusivity of tectonic coal more than that of intact coal. This verified the pore structure experimental results. A simplified illustration of the methane migration before and after ScCO₂ treatment was proposed to analyze the influence of ScCO₂ on the tectonic coal reservoir's CBM. Hence, the results of this study may provide new insights into CO₂-ECBM in tectonic coal reservoirs.

Keywords: supercritical CO₂; tectonic coal; pore structure; methane desorption

1. Introduction

As a major greenhouse gas, CO₂ causes global warming and initiated a series of negative effects on the balance of the natural ecosystem and the sustainable development of human society [1–7]. To mitigate CO₂ emissions into the atmosphere, enhanced coalbed methane recovery with CO₂ sequestration (CO₂-ECBM) is considered to be a promising technology, and it receives widespread attention [8–12]. This technology can not only provide CO₂ storage, but can also enhance the production of coalbed methane (CBM). To date, many scholars proved the feasibility of injecting CO₂ into methane-bearing coal seams using various experimental methods and field tests. Fulton et al. observed that the recovery of CH₄ after CO₂ injection was 57% higher than that of natural emissions [13]. Reznik et al., Jessen et al., and Dutka et al. also verified that CO₂ injection could contribute to the improvement of CH₄ recovery [14–16]. In 1996, the San Juan Basin was selected as

the first demonstration site for CO₂-ECBM. After CO₂ injection, CBM production was increased by five times, and the recovery of CH₄ reached 77–95%, lasting for over six years [17].

The coal seams most suitable for CO₂ sequestration are commonly more than 800 m deep, and the temperature and pressure in coal seams at the most suitable depths are, in many cases, above the critical point for CO₂ (critical temperature and pressure: 31.05 °C and 7.39 MPa) [18]. Numerous studies were undertaken to better understand the interaction between supercritical CO₂ (ScCO₂) and intact coal. When coal is exposed to ScCO₂, the ScCO₂ is incorporated into the coal and it rearranges the coal's structure [19]. It is generally agreed that ScCO₂ can change the pore morphology of coal irreversibly, including pore volume, pore size distribution, surface area, and pore connectivity [20,21]. Additionally, ScCO₂ is an organic solvent and can mobilize some of the organic matter in the coal. If some of the CO₂ is dissolved in the reservoir water, the pH decreases and the CO₂-enriched solution can dissolve some of the minerals present [22–24]. Studies also showed that CO₂ adsorption can cause the coal's matrix to swell [25]. However, the above studies were all focused on the effects of ScCO₂ on intact coal, and there was little research on tectonic coal–ScCO₂ interactions.

Tectonic coal is deformed, sheared coal. The deformation and shearing was caused by tectonism that occurred long after coal formation and diagenesis of the coal seams [26]. Tectonic coal is present all over the world, and there is substantial tectonized coal in China [27,28]. The existence of tectonic coal in some coalfields complicates safe and efficient CO₂ sequestration. This is because the physical and chemical properties of tectonic coal differ from those of intact coal. Additionally, the permeability of tectonic coal is much lower than that of intact coal. This leads to the formation of CBM-rich coals; thus, tectonic coals have huge CBM exploitation potential. However, a CBM extraction well drilled in an area hosting significant tectonic coal may seriously restrict CBM production because the tectonic coal's low permeability restricts gas desorption and migration [29,30]. Therefore, in such an area, CO₂-ECBM is likely to be the technique implemented to solve this problem.

The coal's pore structure affects gas adsorption, diffusion, and seepage. Previous studies [31,32] showed that the pore structure in intact coal and tectonic coal are different and affect how gas desorbs from these coals. These differences are important when the subject of long-term CO₂ storage in coal seams is considered. However, limited research focused on this topic, especially the comprehensive and systematic analysis of the differences of pore structures and gas desorption properties between intact coal and tectonic coal during CO₂-ECBM. Therefore, a better understanding of the pore morphologies and desorption in intact and tectonic coals after ScCO₂ treatment is of significance for CO₂-ECBM in tectonic coal reservoirs.

In this study, the effects of ScCO₂ on the pore structures of intact and tectonic coals was studied using mercury intrusion porosimetry (MIP) and N₂ (77 K) adsorption experiments. Additionally, gas desorption of intact and tectonic coals after ScCO₂ treatment was analyzed using methane desorption experiments. The main focus of this study was the analysis of the pore structures and gas desorption properties of intact and tectonic coals before and after ScCO₂ treatment, and results were compared to analyze the influence of tectonic coal on the CO₂-ECBM process.

2. Materials and Methods

2.1. Coal Samples

Both the intact coal and tectonic coal samples used in the experiments were collected from the Shanxi Formation #3 coal seam in the Sihe coal mine. This mine is in the southern Qinshui basin in Shanxi Province, China (Figure 1). The southern Qinshui basin is not only a major CBM production area, but also the area in which China first carried out a pilot CO₂-ECBM project [33]. The coal samples for this study were collected from fresh working faces in the mine. The samples were then immediately sealed, packed, and sent to the laboratory with minimal delay to prevent oxidation. At the laboratory, standard crushing and screening equipment was used to crush and screen the coal samples to different particle sizes for the different experiments. For each experiment, the crushed and sieved intact coal and

the tectonic coal sub-samples were divided into two fractions for comparative analyses: one fraction was treated with ScCO_2 , and the other was not treated. Selected properties of the intact coal and the tectonic coal are listed in Table 1. Compared with intact coal, the mineral content and Langmuir volume of the tectonic coal is greater, indicating that tectonic coal contains more minerals and can absorb more methane. The moisture, ash, and $R_{0, \max}$ values of the tectonic coal are slightly higher than those of the intact coal.

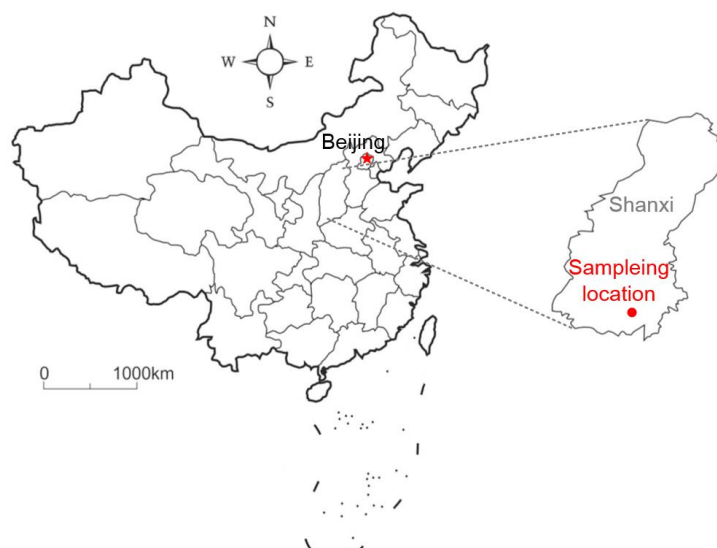


Figure 1. Map showing the location of the Sihe coal mine, the mine from which the samples were collected.

Table 1. Maximum vitrinite reflectances, Langmuir volume and pressure, macerals, and partial proximate analyses for the coal samples used in this study.

Samples	Type	$R_{0, \max}$ (%)	Langmuir Volume	Langmuir Pressure	Proximate Analysis (wt.%)			Macerals (vol.%)		
					M_{ad} (%)	A_{ad} (%)	V_{daf} (%)	V (%)	I (%)	M (%)
Intact coal	Anthracite	3.13	45.83	0.81	1.35	14.26	8.46	79.70	17.22	3.08
Tectonic coal		3.26	48.77	0.89	1.58	17.09	8.24	76.42	16.72	6.86

$R_{0, \max}$, maximum vitrinite reflectance; M_{ad} , moisture content; A_{ad} , ash yield; V_{daf} , volatile matter. The subscript “ad” stands for air-dried basis. V, vitrinite; I, inertinite; M, mineral.

2.2. Experimental Methods

For this study, MIP, N_2 (77 K) adsorption, and methane desorption experiments on both intact and tectonic coal specimens with and without ScCO_2 treatment were conducted.

A schematic of the set-up used for the ScCO_2 treatment is shown in Figure 2. According to the pressure gradient and temperature gradient in the southern Qinshui basin, the temperature of the reservoir is $35\text{ }^\circ\text{C}$ and the pressure is 8 MPa at the depth of 800 m. Therefore, $35\text{ }^\circ\text{C}$ and 8 MPa were chosen as the treatment conditions to replicate the in situ conditions. Before the ScCO_2 treatment, coal samples were first degassed in a vacuum chamber at $50\text{ }^\circ\text{C}$ and 4 Pa for 24 h. Then, the constant temperature bath was set to $35\text{ }^\circ\text{C}$ and the sample tank was filled with CO_2 using an ISCO pump. Subsequently, the pressure was maintained at 8 MPa for 72 h, and the constant temperature bath was held at $35\text{ }^\circ\text{C}$.

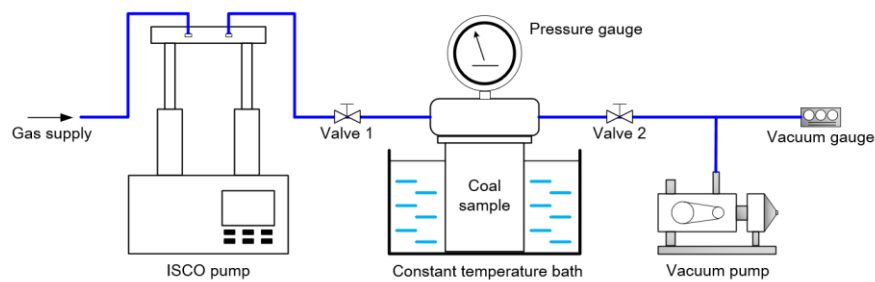


Figure 2. Schematic diagram showing the set-up used for the supercritical CO₂ treatments.

The pore structure of both ScCO₂-treated and untreated coal samples was analyzed using a PM33-GT-12 mercury porosimeter. This instrument can measure pore diameters between 0.007 and 1000 μm over a pressure range of 1.5–231,000 kPa. The porosimetry data were modeled using the Washburn Equation [34]:

$$r = \frac{2\sigma \cos \theta}{p_c}, \quad (1)$$

where r is the pore radius of the porous material (nm), σ is the surface tension of mercury (dyn/cm²), θ is the contact angle between mercury and the porous material's surface (°), and p_c is the capillary pressure (MPa).

The pore size distribution (PSD) was determined using the N₂ (77 K) adsorption method employing a Quadrasorb SI instrument. The N₂ adsorption–desorption isotherms of ScCO₂-treated and untreated coal samples were obtained at a temperature of −196 °C with a relative pressure (p/p_0) range of 0.01–0.99. The Barrett-Joyner-Halenda (BJH) method was used to calculate total pore volume (TPV), density functional theory (DFT) was used to calculate PSD, and the Brunauer-Emmett-Teller (BET) method was used to calculate the specific surface area (SSA) [35–37].

Methane desorption data from both treated and untreated intact and tectonic coals were collected during the gas desorption experiments. The experiments were run according to China National Standards AQ/T 1065-2008 and GB 474-2008; the experimental set-up is shown in Figure 3. Coal particles from 1 to 3 mm in diameter were placed in a container and degassed at 50 °C and 4 Pa for 24 h. After degassing, the container, in a 30 °C water bath, was quickly filled with 99.9% pure methane to achieve the methane adsorption equilibrium (2 MPa and 4 MPa). When adsorption equilibrium was reached, valve 4 was opened to vent all the free methane from the container. The container was then connected to the gas desorption measuring cylinder for the gas desorption experiment. During the experiment, the volume of methane desorbed was recorded at specific times; the desorption segment of each experiment lasted two hours.

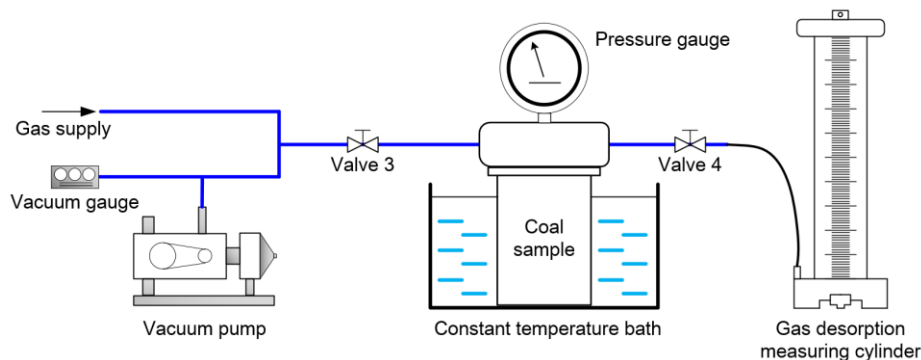


Figure 3. Schematic diagram showing the set-up used for the gas desorption experiments.

The whole experimental process is shown in Figure 4.

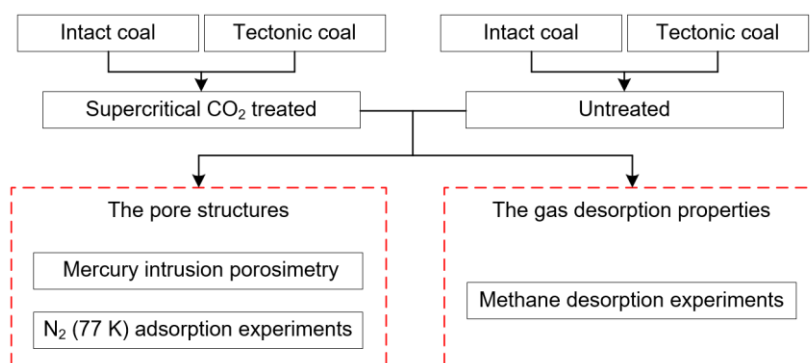


Figure 4. The whole experimental process.

3. Results and Discussion

3.1. Pore Structure Analysis

3.1.1. Pore Size Distribution

To analyze the MIP data from treated and untreated intact and tectonic coal samples quantitatively, the Hodot classification for coal pore sizes was used. This classification scheme divides the pores into macropores (>1000 nm), mesopores (100–1000 nm), transition pores (10–100 nm), and micropores (<10 nm) [38].

Figure 5 shows the PSDs for both ScCO₂-treated and untreated coal samples. It is clear from the figure that the macropores and mesopores in the tectonic coal were more developed. This effect was reported by a number of previous studies [39,40]. It is interesting to note that the macropores and mesopores in the tectonic coal were obviously larger after ScCO₂ treatment, and the effect of the ScCO₂ treatment on the tectonic coal's pores was greater than its effect on the intact coal's pores. According to the data in Table 2, the proportion of macropores and mesopores in the tectonic coal was 33.74% before ScCO₂ treatment, but 36.02% after treatment, greater than the pore percentages in the intact coal (15.91% before and 21.37% after). It can be deduced that ScCO₂ treatment may observably promote the development of mesopores and macropores of tectonic coal. The data also show that the porosity of the treated intact and tectonic coal samples increased by 18.90% (from 4.18% to 4.97%) and 23.14% (from 5.23% to 6.44%), respectively. Previous studies [22,23,41] showed that ScCO₂ can mobilize some of the polycyclic aromatic hydrocarbons and aliphatic hydrocarbons in the coal. Additionally, CO₂ will form carbonic acid when it is dissolved in the water in the coal seams, and this acid can dissolve some of the inorganic minerals in the coal, such as calcites, dolomites, and magnesites [42]. This may result in increased pore sizes. Additionally, Cao et al. found that the mean extraction yield of the tectonic coal was 1.45% using organic solvent, whereas that of the intact coal was 0.44% [43]. Apparently, the mobilizing effect in tectonic coal is more pronounced than its effect in intact coal. These MIP data show that the changes in PSD for the transition pores and micropores were less significant. To investigate the PSDs of the smaller pores in more detail, additional analyses were performed using N₂ (77 K) adsorption.

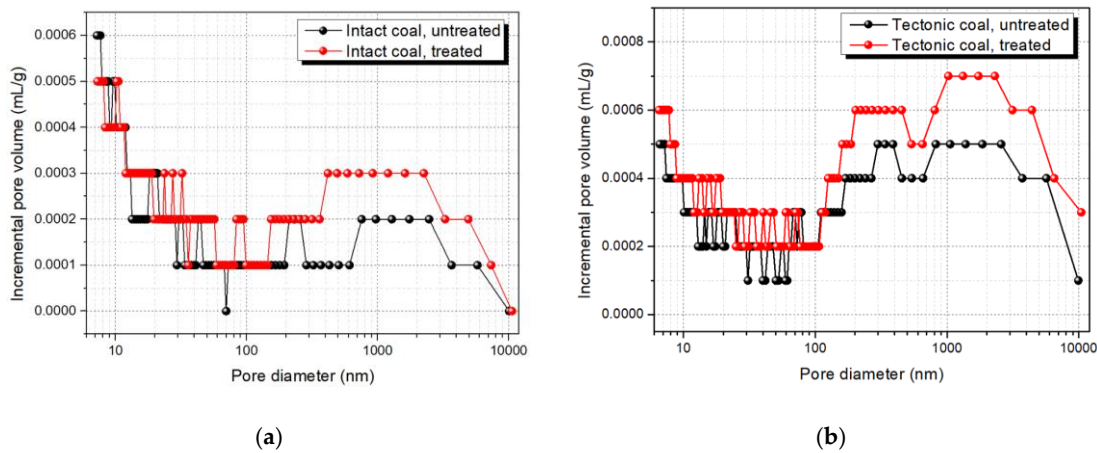


Figure 5. Pore size distributions determined by mercury intrusion porosimetry (MIP) for samples of (a) intact coal and (b) tectonic coal with and without supercritical CO₂ (ScCO₂) treatment.

Table 2. Mercury intrusion porosimetry porosities and pore volume distributions for supercritical CO₂ (ScCO₂)-treated and untreated coal samples.

Sample	Porosity (%)	Pore Volume Distribution (%)			
		V ₁ /V _t	V ₂ /V _t	V ₃ /V _t	V ₄ /V _t
Intact coal, untreated	4.18	27.73	56.36	12.27	3.64
Intact coal, treated	4.97	20.23	58.40	16.03	5.34
Tectonic coal, untreated	5.23	19.63	46.63	24.85	8.90
Tectonic coal, treated	6.44	19.43	44.55	24.88	11.14

V₁ = pore volume of micropores; V₂ = pore volume of transition pores; V₃ = pore volume of mesopores; V₄ = pore volume of macropores; V_t = total pore volume.

Using the N₂ (77 K) manometric adsorption technique can avoid the destruction of pores under high pressure; thus, it is commonly used for PSD measurements of smaller pores [26]. As shown in Figure 6, after ScCO₂ treatment, the PSDs for small pores were not significantly affected, although a slight tendency for pore sizes to increase could be discerned. This is consistent with the MIP results. The PSDs of both the treated and the untreated intact and tectonic coals had two peaks in the portion of the isotherm, representing pores with diameters smaller than 10 nm, indicating that the micropore structure of these coal samples was relatively developed.

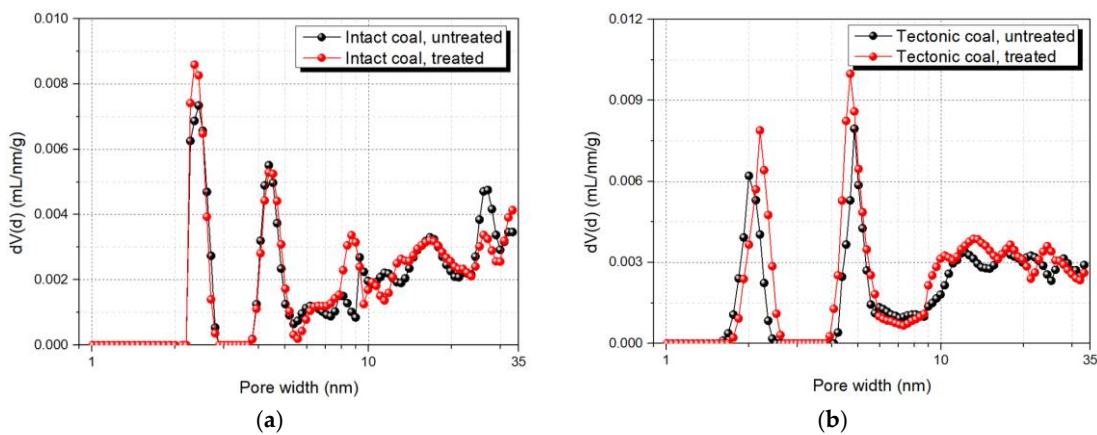


Figure 6. Pore size distributions of the untreated and ScCO₂-treated coal samples as determined by the density functional theory (DFT) analyses of N₂ (77 K) adsorption isotherms for (a) intact coal and (b) tectonic coal.

3.1.2. Pore Volume and Surface Area

Table 3 summarizes the changes in the TPVs and SSAs for untreated and ScCO₂-treated intact and tectonic coal samples. Overall, the BJH-TPVs and the BET-SSAs (the values determined by N₂ (77 K) adsorption) showed a slight increase after ScCO₂ treatment; the TPVs and SSAs determined by MIP showed a more significant increase. These increases are consistent with the PSD results. Additionally, the TPVs and SSAs of both the treated and untreated tectonic coal samples were higher than those for the intact coal samples. A study by Qu et al. [44] explained this point very well, and suggested that the tectonism that the coal underwent greatly promoted the fracture of macromolecular chains and aromatic layers, which was conducive to the development of molecular structural disorder in the coal. This led to increased pore volume and, hence, increased surface area.

Table 3. Total pore volumes and specific surface areas for untreated and ScCO₂-treated intact and tectonic coal samples.

Sample	BJH-TPV (mL/g)	BET-SSA (m ² /g)	MIP-TPV (mL/g)	MIP-SSA (m ² /g)
Intact coal, untreated	0.015	3.421	0.0220	0.165
Intact coal, treated	0.016	3.862	0.0262	0.190
Tectonic coal, untreated	0.019	3.964	0.0326	0.214
Tectonic coal, treated	0.021	4.402	0.0422	0.256

BET, Brunauer-Emmett-Teller; BJH, Barrett-Joyner-Halenda; SSA, specific surface area; TPV, total pore volume. The BJH-TPV and BET-SSA values are from N₂ (77 K) adsorption determinations.

3.1.3. Pore Connectivity

The pores in coal can be divided into four types according to their shapes: cross-linked, passing, dead end, and closed pores. The first three types are called open pores [45]. Some useful information about the pores can be extracted from the MIP injection/ejection curves and the hysteresis loops. As shown in Figure 7, after ScCO₂ treatment, the mercury injection volumes for the intact coal and the tectonic coal increased by 19.09% (from 0.0220 to 0.0262 mL/g) and 29.45% (from 0.0326 to 0.0422 mL/g), respectively. The mercury withdrawal volume for these two coals showed the same trend, increasing by 9.14% (from 0.0197 to 0.0215 mL/g) and 17.42% (from 0.0264 to 0.0310 mL/g), indicating that the open pore volume increased after ScCO₂ treatment [46]. Moreover, the hysteresis loops of all treated coals increased, indicating that the pore network was more complex with more bottleneck pores, and there was an increase in the number of open pores [47]. Thus, the connectivity of the treated tectonic coal sample was excellent, which may affect the methane desorption, diffusion, and seepage.

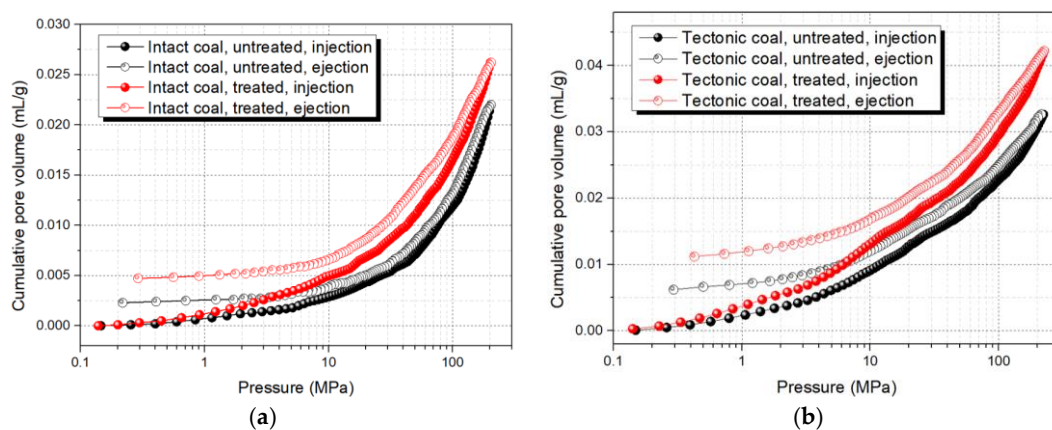


Figure 7. Mercury intrusion porosimetry injection and ejection curves for untreated and treated coal samples: (a) intact coal; (b) tectonic coal.

3.2. Desorption Analysis

Carbon dioxide sequestration in coal seams enhances CBM production. Simplistically, CO₂ sequestration can be thought of as just gas in/gas out: carbon dioxide seepage, diffusion, and adsorption in, coupled with methane desorption, diffusion, and seepage out. The preceding pore structure analysis showed that ScCO₂ can change the pore structure in intact and tectonic coals, and this will undoubtedly affect the desorption, diffusion, and seepage of the methane. Previous studies showed that the diffusion of methane through the coal's matrix has an important influence on CBM production [48,49]. However, research on how ScCO₂ affects methane diffusion in tectonic coal is still limited. Therefore, the methane desorption from ScCO₂-treated intact and tectonic coals was analyzed.

3.2.1. Gas Desorption Curves

Methane desorption curves for untreated and treated coal samples are shown in Figure 8. The cumulative desorption volume increased as the desorption time increased. The slopes of the desorption curves were steepest in the early stages of the desorption experiments, and the slopes gradually decreased with time. Compared with intact coal, the slopes of the desorption curves of tectonic coal were greater. This is because the mesopores and macropores of tectonic coal were more developed. When the adsorption equilibrium pressure was 4 MPa, the volumes of gas desorbed from the coal samples were higher than the volumes of gas desorbed when the adsorption equilibrium pressure was 2 MPa. This is because, during adsorption, the coal matrix could absorb more methane at higher equilibrium pressures [50].

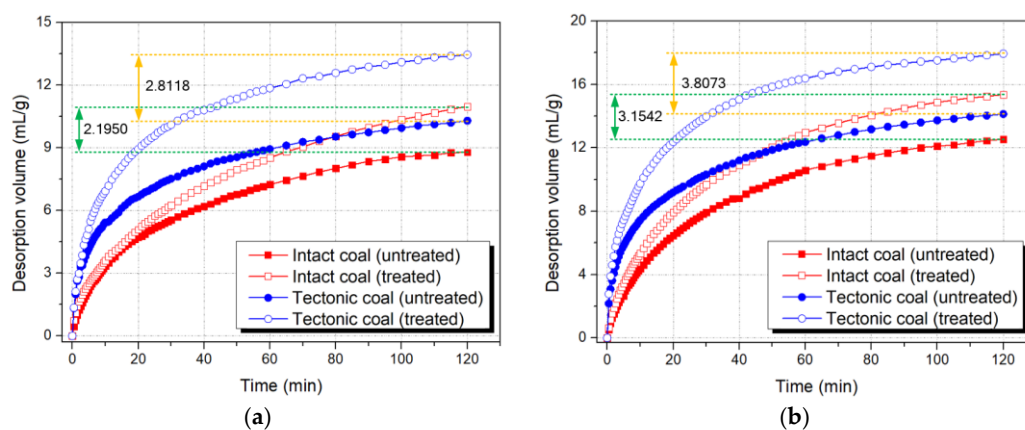


Figure 8. Methane desorption curves for untreated and ScCO₂-treated coal samples: (a) 2 MPa; (b) 4 MPa.

In general, ScCO₂ treatment has a considerable effect on the coal sample's gas desorption. As shown in Figure 7, when the equilibrium pressure was 4 MPa and 2 MPa, the final desorption volume of treated tectonic coal increased by 2.8118 mL/g and 3.8073 mL/g, respectively. However, under the same conditions, the final volume of gas desorbed from treated intact coal was slightly greater than volume of gas desorbed from untreated tectonic coal (2.1950 mL/g and 3.1542 mL/g). The final desorption volume for treated tectonic coal was 1.33 to 1.40 times that of the desorption volume for intact coal. These results indicate that more CBM can be extracted from a tectonic coal CBM reservoir after the coal in the reservoir is injected with ScCO₂.

To further analyze the changes in gas desorption from ScCO₂-treated intact and tectonic coal, their gas diffusion coefficients were compared in the subsequent section.

3.2.2. Gas Desorption Diffusion Coefficients

Based on Fick's diffusion laws, an analytic solution for a diffusion equation was presented by Crank [51] under Dirichlet boundary conditions (Equation (2)). However, this analytical solution is difficult to apply to practical engineering problems because it is in the form of an infinite series. Yang [52] simplified Equation (1) to a more practical form (Equation (3)), and this equation is widely used in engineering and can represent coal's gas desorption very well. The two equations are as follows:

$$\frac{Q_t}{Q_\infty} = 1 - \frac{6}{\pi^2} \sum_{n=1}^{\infty} \frac{1}{n^2} e^{-\frac{Dn^2\pi^2t}{r_c^2}}, \quad (2)$$

$$\frac{Q_t}{Q_\infty} = \sqrt{1 - e^{-B_1t}}, \quad (3)$$

where D is a diffusion coefficient, t is the desorption time, r_c is the average particle diameter, Q_t is the cumulative desorption amount at time t , Q_∞ is the ultimate desorption amount, and B_1 is a fitting parameter related to the diffusion coefficient D and the average diameter r_c , which can be calculated from $B_1 = K(4\pi^2D)/r_c^2$. K is a correction parameter commonly taken to be equal to 1.

The variable Q_∞ is, in most cases, calculated using Equation (4) [53].

$$Q_\infty = \left(\frac{V_L P_{eq}}{P_L + P_{eq}} - \frac{V_L P_a}{P_L + P_a} \right) (1 - M_{ad} - A_{ad}), \quad (4)$$

where P_{eq} is the definite equilibrium pressure, P_a is the atmospheric pressure, M_{ad} is the moisture content, and A_{ad} is the ash content of the coal samples.

Equations (3) and (4) can be used to calculate the diffusion coefficients for the coals used in this study using the data from the methane desorption curves in Figure 7 as input parameters. The results are shown in Table 4.

Table 4. Gas diffusion coefficients for supercritical CO₂-treated and untreated tectonic and intact coals.

Samples	Intact Coal			Tectonic Coal			Pressure
	Untreated	Treated	Change	Untreated	Treated	Change	
D ($\times 10^{-12}$ m ² /s)	2.6360	3.8480	45.98%	3.9991	7.5020	87.59%	2 MPa
	4.2155	6.0091	42.55%	5.2912	9.8848	86.82%	4 MPa

According to the results listed in Table 4, it is clear that ScCO₂ treatment considerably increased the tectonic coal's diffusion coefficient, and the treatment increased the tectonic coal's diffusion coefficient more than it increased the coefficient for intact coal. For example, when the equilibrium pressure was 2 MPa, ScCO₂ treatment increased the diffusion coefficient for treated tectonic coal by 87.59%, but the treatment only increased intact coal's diffusion coefficient by 45.98%. It can also be seen in Table 4 that, under the same conditions, tectonic coal's diffusion coefficients were higher than those for intact coal. This is because desorption largely depends on the properties of the pores and the pore structure in the coal. As indicated by the MIP test results, the proportion of macropores and mesopores increased after ScCO₂ treatment, especially for tectonic coal, and larger pores can provide better channels for gas migration. In short, tectonic coal has stronger diffusivity capacity.

3.2.3. Implication for CO₂-ECBM in Tectonic Coal Reservoirs

Liu et al. surveyed the distribution of tectonic coal reservoirs in China and indicated that the CBM resource in these reservoirs was as much as 5.60 trillion cubic meters. This amounts to 39.20% of China's CBM resources [54]. Although the tectonic coal reservoirs have great potential for CBM development, the permeability of this type of gas reservoir is very low. This means that developing the resources in these CMB reservoirs would be very difficult.

A simplified illustration of the migration of methane in a coal seam is shown in Figure 9. In Figure 9, methane migration is divided into three stages: desorption, diffusion, and seepage. Red circles represent adsorbed methane in the coal matrix, green circles represent free methane, yellow squares represent the coal skeleton, and purple squares represent pores in the matrix. In tectonic coal reservoirs, gas migration to the fractures is slow because of the tectonic coal's low permeability. Therefore, only a small amount of methane can flow to CBM wells and the production of CBM is low (Figure 9, untreated). The results of the methane desorption experiments described in previous sections show that both the desorption capacities and diffusion coefficients of treated coals were higher than in untreated coals. Therefore, more adsorbed methane was desorbed from the coal's matrix and diffused to the fractures after CO₂ was injected into the tectonic coal reservoir (Figure 9, treated). The pressure gradient must increase when more free methane is present in the fractures, as shown in Figure 9, treated (more green circles exist in the fracture). According to Darcy's law, an increasing pressure gradient must lead to an increase in gas flow per unit time; thus, more methane will flow to CBM wells. Additionally, the pore structure analysis described in Section 3.1 indicated that the number of the macropores and mesopores of the coal increased after ScCO₂ treatment, which provides more space for gas migration and improves the absolute permeability of coal seams to some extent. Furthermore, Liu et al. (2018) demonstrated that CBM production was mainly controlled by diffusion after six days of extraction when the diffusion coefficient was 1×10^{-12} m²/s [49]. Therefore, a higher diffusion coefficient has a positive effect on CBM production. In short, CO₂-ECBM could overcome the negative effects of low permeability in tectonic coal reservoirs to some extent, thereby promoting CBM development.

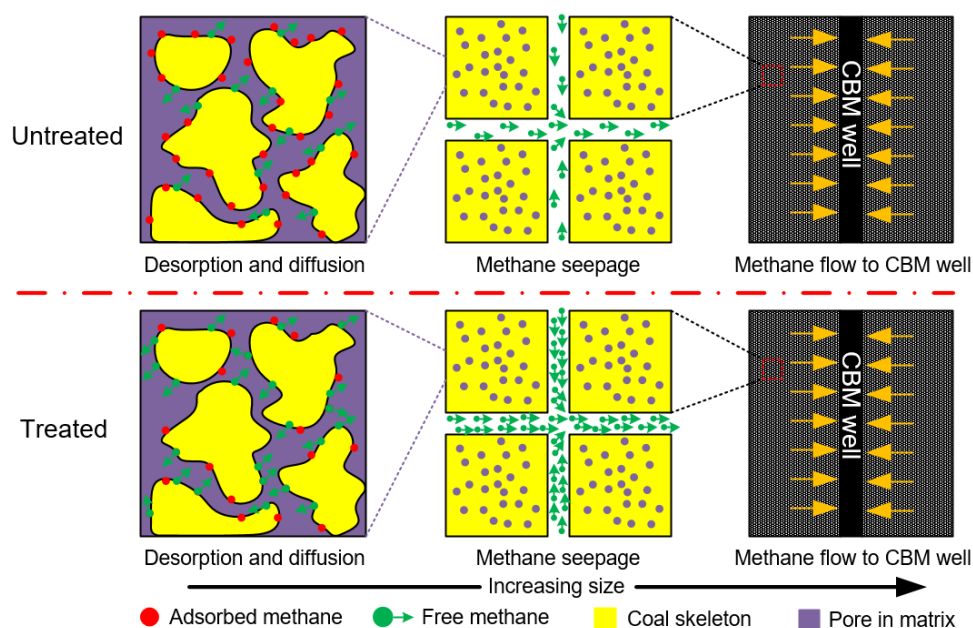


Figure 9. Sketch showing methane migration in untreated and treated coal.

4. Conclusions

This study investigated changes in the pore structures of intact coal and tectonic coal after ScCO₂ treatment using mercury intrusion porosimetry and N₂ (77 K) adsorption, and determined the effects of these changes on the coal's gas desorption and diffusion properties. The changes in desorption and diffusion were used to study the implications for enhanced coalbed methane recovery with CO₂ sequestration in tectonic coal reservoirs. The experimental results suggest the following conclusions:

- (1) Compared with intact coal, the macropores and mesopores in tectonic coal were obviously larger after ScCO₂ treatment. Additionally, the TPV, SSA, and pore connectivity of treated tectonic coal were significantly improved. Pore structure analysis showed that tectonic coal was significantly

affected by ScCO₂ treatment. This was because tectonic coal contained more minerals and the mobilizing effect in tectonic coal was more pronounced.

- (2) The results of the methane desorption experiment showed that the desorption capacity of intact coal and tectonic coal was improved to a certain extent by ScCO₂ treatment; however, the diffusion coefficient of the treated tectonic coal increased twice as much as that of intact coal. This change was consistent with the pore structure experimental results. The enhancement of the tectonic coal's diffusion capacity after ScCO₂ treatment can partially overcome the limitation imposed on tectonic coal reservoir CBM development by the coal's inherent low permeability. The results of this study may provide new insights into CO₂-ECBM in tectonic coal reservoirs.

Author Contributions: E.S. and Y.L. conceived and designed the experiments. E.S. and L.L. performed the experiments. E.S. and Q.Z. analyzed the data. E.S. and F.N. wrote the paper.

Funding: This work was financially supported by the National Science and Technology Major Project of China (Grant No. 2016ZX05043005 and 2016ZX05045004), the State Key Research Development Program of China (Grant No. 2016YFC0801404 and 2016YFC0801402), and the National Natural Science Foundation of China (51674050 and 51704046), which are gratefully acknowledged.

Acknowledgments: The authors thank the editor and anonymous reviewers for their valuable advice. The authors thank David Frishman, PhD, from Liwen Bianji, Edanz Group China (www.liwenbianji.cn/ac), for editing the English text of a draft of this manuscript.

Conflicts of Interest: The authors declare no conflicts of interest.

References

1. Zou, Q.; Lin, B.; Zheng, C.; Hao, Z.; Zhai, C.; Liu, T.; Liang, J.; Yan, F.; Yang, W.; Zhu, C. Novel integrated techniques of drilling-slotting-separation-sealing for enhanced coal bed methane recovery in underground coal mines. *J. Nat. Gas Sci. Eng.* **2015**, *26*, 960–973. [[CrossRef](#)]
2. Gale, W. A review of energy associated with coal bursts. *Int. J. Min. Sci. Technol.* **2018**, *28*, 755–761. [[CrossRef](#)]
3. Yu, G.; Zhai, C.; Qin, L.; Tang, Z.; Wu, S.; Xu, J. Changes to coal pores by ultrasonic wave excitation of different powers. *J. China Univ. Min. Technol.* **2018**, *47*, 264–270.
4. Liu, C.; Li, S.; Yang, S. Gas emission quantity prediction and drainage technology of steeply inclined and extremely thick coal seams. *Int. J. Min. Sci. Technol.* **2018**, *28*, 415–422.
5. Liang, B.; Jia, L.; Sun, W.; Jiang, Y. Experimental on the law of coal deformation and permeability under desorption and seepage. *J. China Univ. Min. Technol.* **2018**, *47*, 935–941.
6. Chang, K.; Tian, H. Technical scheme and application of pressure-relief gas extraction in multi-coal seam mining region. *Int. J. Min. Sci. Technol.* **2018**, *28*, 483–489.
7. Zou, Q.; Lin, B. Fluid–solid coupling characteristics of gas-bearing coal subjected to hydraulic slotting: An experimental investigation. *Energy Fuels* **2018**, *32*, 1047–1060. [[CrossRef](#)]
8. White, C.M.; Smith, D.H.; Jones, K.L.; Goodman, A.L.; Jikich, S.A.; LaCount, R.B.; DuBose, S.B.; Ozdemir, E.; Morsi, B.I.; Schroeder, K.T. Sequestration of carbon dioxide in coal with enhanced coalbed methane recovery: A review. *Energy Fuels* **2005**, *19*, 659–724. [[CrossRef](#)]
9. Haszeldine, R.S. Carbon capture and storage: How green can black be? *Science* **2009**, *325*, 1647–1652. [[CrossRef](#)]
10. Zhang, X.; Ranjith, P.G.; Perera, M.S.A. Gas transportation and enhanced coalbed methane recovery processes in deep coal seams: A review. *Energy Fuels* **2016**, *30*, 8832–8849. [[CrossRef](#)]
11. Gale, J. Geological storage of CO₂: What do we know, where are the gaps and what more needs to be done? *Energy* **2004**, *29*, 1329–1338. [[CrossRef](#)]
12. Perera, M. A Comprehensive Overview of CO₂ Flow Behaviour in Deep Coal Seams. *Energies* **2018**, *11*, 906. [[CrossRef](#)]
13. Fulton, P.F.; Parente, C.A.; Rogers, B.A.; Shah, N.; Reznik, A. A laboratory investigation of enhanced recovery of methane from coal by carbon dioxide injection. In *SPE Unconventional Gas Recovery Symposium*; Society of Petroleum Engineers: Pittsburgh, PA, USA, 1980.
14. Reznik, A.A.; Singh, P.K.; Foley, W.L. An analysis of the effect of CO₂ injection on the recovery of in-situ methane from bituminous coal: An experimental simulation. *Soc. Petrol. Eng. J.* **1984**, *24*, 521–528. [[CrossRef](#)]

15. Jessen, K.; Tang, G.-Q.; Kovscek, A.R. Laboratory and simulation investigation of enhanced coalbed methane recovery by gas injection. *Transp. Porous Media* **2008**, *73*, 141–159. [[CrossRef](#)]
16. Dutka, B.; Kudasik, M.; Pokryszka, Z.; Skoczylas, N.; Topolnicki, J.; Wierzbicki, M. Balance of CO₂/CH₄ exchange sorption in a coal briquette. *Fuel Process. Technol.* **2013**, *106*, 95–101. [[CrossRef](#)]
17. Stevens, S.H.; Kuuskraa, V.A.; Spector, D.; Riemer, P. CO₂ sequestration in deep coal seams: Pilot results and worldwide potential. In Proceedings of the Greenhouse Gas Control Technology, Saskatoon, SK, Canada, 4–6 October 1999; pp. 175–180.
18. Span, R.; Wagner, W. A new equation of state for carbon dioxide covering the fluid region from the triple-point temperature to 1100 K at pressures up to 800 MPa. *J. Phys. Chem. Ref. Data* **1996**, *25*, 1509–1596. [[CrossRef](#)]
19. Larsen, J.W. The effects of dissolved CO₂ on coal structure and properties. *Int. J. Coal Geol.* **2004**, *57*, 63–70. [[CrossRef](#)]
20. Zhang, K.; Cheng, Y.; Jin, K.; Guo, H.; Liu, Q.; Dong, J.; Li, W. Effects of Supercritical CO₂ Fluids on Pore Morphology of Coal: Implications for CO₂ Geological Sequestration. *Energy Fuels* **2017**, *31*, 4731–4741. [[CrossRef](#)]
21. Chen, R.; Qin, Y.; Wei, C.; Wang, L.; Wang, Y.; Zhang, P. Changes in pore structure of coal associated with Sc-CO₂ extraction during CO₂-ECBM. *Appl. Sci.* **2017**, *7*, 931. [[CrossRef](#)]
22. Liu, C.J.; Wang, G.X.; Sang, S.X.; Rudolph, V. Changes in pore structure of anthracite coal associated with CO₂ sequestration process. *Fuel* **2010**, *89*, 2665–2672. [[CrossRef](#)]
23. Kolak, J.J.; Hackley, P.C.; Ruppert, L.F.; Warwick, P.D.; Burruss, R.C. Using ground and intact coal samples to evaluate hydrocarbon fate during supercritical CO₂ injection into coal beds: Effects of particle size and coal moisture. *Energy Fuels* **2015**, *29*, 5187–5203. [[CrossRef](#)]
24. Zhang, D.; Gu, L.; Li, S.; Lian, P.; Tao, J. Interactions of supercritical CO₂ with coal. *Energy Fuels* **2013**, *27*, 387–393. [[CrossRef](#)]
25. Busch, A.; Gensterblum, Y. CBM and CO₂-ECBM related sorption processes in coal: A review. *Int. J. Coal Geol.* **2011**, *87*, 49–71. [[CrossRef](#)]
26. Cai, Y.; Liu, D.; Pan, Z.; Yao, Y.; Li, J.; Qiu, Y. Pore structure and its impact on CH₄ adsorption capacity and flow capability of bituminous and subbituminous coals from Northeast China. *Fuel* **2013**, *103*, 258–268. [[CrossRef](#)]
27. Lu, S.Q.; Cheng, Y.P.; Li, W.; Wang, L. Pore structure and its impact on CH₄ adsorption capability and diffusion characteristics of normal and deformed coals from Qinshui Basin. *Int. J. Oil Gas Coal Technol.* **2015**, *10*, 76–78. [[CrossRef](#)]
28. Ju, Y.W.; Jiang, B.; Hou, Q.L.; Wang, G.L. The new structure-genetic classification system in tectonically deformed coals and its geological significance. *J. China Coal Soc.* **2004**, *29*, 513–517.
29. Shi, J.Q.; Durucan, S. A bidisperse pore diffusion model for methane displacement desorption in coal by CO injection. *Fuel* **2003**, *82*, 1219–1229. [[CrossRef](#)]
30. An, F.H.; Cheng, Y.P. An explanation of large-scale coal and gas outbursts in underground coal mines: The effect of low-permeability zones on abnormally abundant gas. *Nat. Hazard Earth Syst.* **2014**, *14*, 4751–4775. [[CrossRef](#)]
31. Clarkson, C.R.; Bustin, R.M. The effect of pore structure and gas pressure upon the transport properties of coal: A laboratory and modeling study. 1. Isotherms and pore volume distributions. *Fuel* **1999**, *78*, 1333–1344. [[CrossRef](#)]
32. Pan, J.; Zhao, Y.; Hou, Q.; Jin, Y. Nanoscale pores in coal related to coal rank and deformation structures. *Transp. Porous Media* **2015**, *107*, 543–554. [[CrossRef](#)]
33. Wong, S.; Law, D.; Deng, X.; Robinson, J.; Kadatz, B.; Gunter, W.D.; Ye, J.; Feng, S.; Fan, Z. Enhanced coalbed methane and CO₂ storage in anthracitic coals—Micro-pilot test at South Qinshui, Shanxi, China. *Int. J. Greenhouse Gas Control* **2007**, *1*, 215–2228. [[CrossRef](#)]
34. Washburn, E.W. The dynamics of capillary flow. *Phys. Rev. Ser.* **1921**, *17*, 273–283. [[CrossRef](#)]
35. Barrett, E.P.; Joyner, L.G.; Halenda, P.P. The determination of pore volume and area distributions in porous substances. I. Computations from nitrogen isotherms. *J. Am. Chem. Soc.* **1951**, *73*, 373–380. [[CrossRef](#)]
36. Brunauer, S.; Emmett, P.H.; Teller, E. Adsorption of gases in multimolecular layers. *J. Am. Chem. Soc.* **1938**, *60*, 309–319. [[CrossRef](#)]
37. Landers, J.; Gor, G.Y.; Neimark, A.V. Density functional theory methods for characterization of porous materials. *Colloids Surf. A* **2013**, *437*, 3–32. [[CrossRef](#)]

38. Hodot, B.B. *Outburst of Coal and Coalbed Gas*; China Industry Press: Beijing, China, 1966.
39. Hou, Q.; Li, H.; Fan, J.; Ju, Y.; Wang, T.; Li, X.; Wu, Y. Structure and coalbed methane occurrence in tectonically deformed coals. *Sci. China Earth Sci.* **2012**, *55*, 1755–1763. [[CrossRef](#)]
40. Li, M.; Jiang, B.; Lin, S.; Lan, F.; Wang, J. Structural controls on coalbed methane reservoirs in faer coal mine, southwest china. *J. Earth Sci.-China* **2013**, *24*, 437–448. [[CrossRef](#)]
41. Perera, M.S.A. Influences of CO₂ injection into deep coal seams: A review. *Energy Fuels* **2017**, *31*, 10324–10334. [[CrossRef](#)]
42. Wellman, T.P.; Grigg, R.B.; Mcpherson, B.J.; Svec, R.K.; Lichtner, P.C. Evaluation of CO₂–brine–reservoir rock interaction with laboratory flow tests and reactive transport modeling. In *International Symposium on Oilfield Chemistry*; Society of Petroleum Engineers: Pittsburgh, PA, USA, 2003.
43. Cao, Y.; Davis, A.; Liu, R.; Liu, X.; Zhang, Y. The influence of tectonic deformation on some geochemical properties of coals—A possible indicator of outburst potential. *Int. J. Coal Geol.* **2003**, *53*, 69–79. [[CrossRef](#)]
44. Qu, Z.; Wang, G.G.X.; Jiang, B.; Rudolph, V.; Dou, X.; Li, M. Experimental study on the porous structure and compressibility of tectonized coals. *Energy Fuels* **2010**, *24*, 2964–2973. [[CrossRef](#)]
45. Rouquerol, F.; Rouquerol, J.; Sing, K. *Adsorption by Powders and Porous Solids*; Academic Press: Cambridge, MA, USA, 2014.
46. Wang, H.; Fu, X.; Jian, K.; Li, T.; Luo, P. Changes in coal pore structure and permeability during N₂ injection. *J. Nat. Gas Sci. Eng.* **2015**, *27*, 1234–1241. [[CrossRef](#)]
47. Guo, H.; Cheng, Y.; Yuan, L.; Wang, L.; Zhou, H. Unsteady-state diffusion of gas in coals and its relationship with coal pore structure. *Energy Fuels* **2016**, *30*, 7014–7024. [[CrossRef](#)]
48. Pan, Z.; Connell, L.D.; Camilleri, M.; Connelly, L. Effects of matrix moisture on gas diffusion and flow in coal. *Fuel* **2010**, *89*, 3207–3217. [[CrossRef](#)]
49. Liu, Z.; Cheng, Y.; Dong, J.; Jiang, J.; Wang, L.; Li, W. Master role conversion between diffusion and seepage on coalbed methane production: Implications for adjusting suction pressure on extraction borehole. *Fuel* **2018**, *223*, 373–384. [[CrossRef](#)]
50. Jiang, H.; Cheng, Y.; Yuan, L. A Langmuir-like desorption model for reflecting the inhomogeneous pore structure of coal and its experimental verification. *RSC. Adv.* **2014**, *5*, 2434–2440. [[CrossRef](#)]
51. Crank, J. Mathematics of Diffusion. In *Handbook of Chemistry Physic*; Oxford University Press: Oxford, UK, 1975.
52. Yang, Q.; Wang, Y. Theory of methane diffusion from coal cuttings and its application. *J. China Coal Soc.* **1986**, *11*, 87–94.
53. Shouqing, L.; Yuanping, C.; Hongxing, Z.; Haijun, G. Gas desorption characteristics of the high-rank intact coal and fractured coal. *Int. J. Min. Sci. Technol.* **2015**, *25*, 819–825.
54. Liu, C.; Zhou, F.; Yang, K.; Xiao, X.; Liu, Y. Failure analysis of borehole liners in soft coal seam for gas drainage. *Eng. Failure Anal.* **2014**, *42*, 274–283. [[CrossRef](#)]

